Journal of Sound and Vibration 329 (2010) 4634–4642

Contents lists available at ScienceDirect

Journal of Sound and Vibration

journal homepage: www.elsevier.com/locate/jsvi

A technique for the *in situ* phase calibration of in-duct axial microphone arrays

C.R. Lowis [a], P.F. Joseph [a,*], P. Sijtsma [b]

[a] Institute of Sound and Vibration Research, University of Southampton, SO17 1BJ, UK
[b] National Aerospace Laboratory NLR, PO Box 153, 8300 AD Emmeloord, The Netherlands

ARTICLE INFO

Article history:
Received 3 February 2009
Received in revised form
22 February 2010
Accepted 27 April 2010
Handling Editor: Y. Auregan
Available online 20 June 2010

ABSTRACT

In aeroengine noise experiments in-duct microphone arrays are often used to make detailed measurements of the sound field transmitted along the duct. The individual microphones in the array must be calibrated with respect to magnitude, and often more critically with respect to phase. Calibration is difficult to perform *in situ* due to the presence of the duct. This paper presents a technique to allow *in situ* phase calibration of axial microphone arrays. It relies on the observation that the measured cross-spectral pressure matrix at the array has a Hermitian Töplitz form in the case where the propagating duct modes are mutually incoherent. Using this property a system of equations can be written which, when solved, allows the phase calibration factors to be obtained. The technique is verified experimentally using a no-flow laboratory rig by comparing the phase calibration factors obtained with those measured in free-field conditions. The accuracy of the phase calibration factors obtained by the technique is limited by the degree of deviation of the measured cross-spectral matrix from Töplitz behaviour. In the experimental results shown this is less than 15° at duct frequencies below $ka=25$. The technique is a robust and rapid method for calibrating in-duct axial microphone arrays.

1. Introduction

Rig-scale tests are often used to study the noise generation of ducted noise sources, such as turbofan engine blades. To understand their noise generation mechanisms engineers have developed various measurement techniques to allow the sound field transmitted along the duct to be quantified in detail. Many of these techniques involve making in-duct measurements of acoustic pressure. Examples of such techniques are modal decomposition [1,2], source location [3], the estimation of far-field directivity [4] and the determination of full source data [5]. A common arrangement of microphones is an array of flush mounted microphones on the wall of the duct such that the microphones themselves do not affect the flow field. The accuracy of such techniques depends critically on the accurate calibration of the microphones, particularly with respect to their phase.

Calibration of microphone sensitivity is typically achieved using a piston-phone. The microphone is placed in a sound field with a known pressure level. The resulting voltage output from the microphone is related to the known level and, by assuming that the microphone has a linear response, the sensitivity (typically expressed in mV/Pa) is determined.

Phase calibration is more difficult. Unless "phase-matched" microphones can be obtained, manufacturing differences between individual microphones cause them to have significantly differing phase responses. To correct for this, each

* Corresponding author.
E-mail addresses: cl@isvr.soton.ac.uk (C.R. Lowis), pfj@isvr.soton.ac.uk (P.F. Joseph), sijtsma@nlr.nl (P. Sijtsma).

0022-460X/$ - see front matter © 2010 Elsevier Ltd. All rights reserved.
doi:10.1016/j.jsv.2010.04.035

microphone is typically placed close to a *reference microphone* in the presence of a broadband sound field. The relative phase response as a function of frequency between the two microphones is then measured. For large arrays, for example those used for mode detection, this is a time consuming process. Moreover for in-duct microphone arrays this technique cannot be performed *in situ*; the microphones must therefore be calibrated outside of the duct. Mounting the microphones in the duct wall after they have been calibrated exposes them to flow and temperature effects. Therefore, changes in the phase response that result from mounting the microphones in the duct are not accounted for in the free-field calibration.

In this paper a calibration technique is proposed that allows the simultaneous *in situ* calibration of in-duct axial microphone arrays. This technique relies on the principle that the phase difference between two microphones in a duct is only a function of their separation distance. This principal holds so long as the individual propagating modes are mutually incoherent. Coherence between modes could occur as a result of the source distribution or reflections from the duct termination. The phase of the measured pressure cross-spectral matrix, $\mathbf{S}_{pp}$, for a microphone array with equally spaced identical sensors, in a such a sound-field is Töplitz. A Töplitz matrix is one in which the elements along each diagonal are identical. In Section 2 we use the expected behaviour of the cross-spectral matrix to set up a system of equations which can be solved to obtain the phase calibration factors. In Section 3 we use a no-flow rig to experimentally validate the technique by comparing the phase calibration factors obtained with those measured in free-field conditions.

2. Theory

In an infinite hard-walled duct of uniform cross-section containing a uniform mean flow and in the absence of reflections from the open end, the acoustic pressure at a single frequency at a particular axial location z_i, can be written as

$$p(\mathbf{x}_i,z_i)=\sum_n a_n(\mathbf{x}_i)\mathrm{e}^{\mathrm{i}k_n(z_s-z_i)} \tag{1}$$

where a_n is the pressure due to the nth mode at the source plane z_s at the position $\mathbf{x}_i$ in the duct cross-section and k_n is the axial mode wavenumber. At positions many wavelengths from the source, the summation is restricted to the propagating modes. The cross-spectrum between two pressure measurements at the same position in the duct cross-section $\mathbf{x}_i$ but at different axial locations i and j is given by

$$S_{p_ip_j}=\lim_{T\to\infty}\frac{\pi}{T}E[p(\mathbf{x}_i,z_i)p^*(\mathbf{x}_i,z_j)] \tag{2}$$

where E is the expectation operator. Substituting Eq. (1) into Eq. (2) and assuming uncorrelated modes, $E[a_n a_{n'}]=0$ for $n\neq n'$ we obtain the result

$$S_{p_ip_j}=\sum_n S_{aa_n}\mathrm{e}^{\mathrm{i}k_n(z_i-z_j)} \tag{3}$$

where

$$S_{aa_n}=\lim_{T\to\infty}\frac{\pi}{T}E[|a_n|^2] \tag{4}$$

is the spectral density of the nth mode amplitude.

Thus, the cross-spectrum of sound pressures between two points, separated axially and well away from the source, depends only on the axial separation distance z_i-z_j between the two points and not on their absolute position. An important condition on Eq. (3) is that reflections from the open end of the duct can be neglected. This is because these reflections can be assumed to be negligible except at very low frequencies, $ka<1$, and at frequencies not too close to the modal cut-on frequencies. The propagating modes in the duct must also be mutually incoherent. This is a valid assumption for the case of broadband aeroengine noise experiments, as demonstrated experimentally by Castres et al. [6], where this technique is envisaged to be most useful.

Assuming the validity of Eq. (3), for an in-duct array of N microphones the measured cross-spectral matrix with elements formed from the individual cross-spectra between each pair of microphones (Eq. (2)), assumed equidistant, has both Hermitian and Töplitz structure, that is, it has the property

$$S_{p_ip_j}=S_{p_kp_l}\quad\text{when } i-j=k-l \tag{5}$$

$$S_{p_ip_j}=S^*_{p_jp_i} \tag{6}$$

For microphones with different amplitude and phase responses the measured cross-spectral matrix, $\tilde{\mathbf{S}}_{pp}$, deviates from the Hermitian Töplitz form. Instead it takes the form

$$\tilde{\mathbf{S}}_{pp}=\Gamma\mathbf{S}_{pp}\Gamma^H \tag{7}$$

where Γ is a diagonal matrix of complex calibration factors with gain, g_i, and a phase, ϕ_i, relative to some arbitrary reference phase,

$$\Gamma=\mathrm{diag}(g_1\mathrm{e}^{\mathrm{i}\phi_1},g_2\mathrm{e}^{\mathrm{i}\phi_2},\ldots,g_N\mathrm{e}^{\mathrm{i}\phi_N}) \tag{8}$$

The phases are defined relative to some undetermined arbitrary phase reference. In effect, therefore, the technique only provides the phase *difference* between different microphones. For an axial array located in an infinite duct the Töplitz structure is expected to be a valid assumption for both the gain and phase components of $\mathbf{S}_{pp}$. In this paper we restrict the technique to phase calibration, since amplitude calibration is more readily performed using, for example, a piston-phone.

We denote the difference in phase between two *identical* microphones i and j, arising entirely from their different locations, by Φ_{ij}, which from Eq. (5) has the property $\Phi_{ij}=\Phi_{kl}$ for $i-j=k-l$. From Eq. (7) the phase of the measured cross-spectral pressure matrix $\tilde{\mathbf{S}}_{pp}$, with calibration factors included, therefore has the form

$$\mathrm{angle}(\tilde{\mathbf{S}}_{pp})=\begin{pmatrix} 0 & \Phi_{12}+\phi_1-\phi_2 & \Phi_{13}+\phi_1-\phi_3 & \cdots & \Phi_{1N}+\phi_1-\phi_N \\ & 0 & \Phi_{23}+\phi_2-\phi_3 & \cdots & \Phi_{2N}+\phi_2-\phi_N \\ & & 0 & \ddots & \vdots \\ & & & 0 & \Phi_{(N-1)N}+\phi_{(N-1)}-\phi_N \\ & & & & 0 \end{pmatrix} \tag{9}$$

where, since $\tilde{\mathbf{S}}_{pp}$ is Hermitian, only the upper triangular half of the matrix is shown for clarity.

By imposing the Töplitz property on the matrix of Eq. (9), i.e. with the correct phase factors incorporated into the phase of the cross-spectral matrix, $\Phi_{ij}=\Phi_{kl}$ when $i-j=k-l$, we can write the system of equations from Eq. (9) as

$$\phi_i-2\phi_{i+1}+\phi_{i+2}=v_i=\mathrm{angle}(\tilde{\mathbf{S}}_{p_ip_{(i+1)}})-\mathrm{angle}(\tilde{\mathbf{S}}_{p_{(i+1)}p_{(i+2)}}) \quad (i=1,2,\ldots,N-2) \tag{10}$$

where v_i is the measured difference in phase between *adjacent* elements in the leading diagonal of $\tilde{\mathbf{S}}_{pp}$. A similar relationship may be written for all the diagonals of $\tilde{\mathbf{S}}_{pp}$.

Note that the left-hand side of Eq. (10) contains only microphone phase calibration factors while the right-hand side contains only measurable phase quantities. The least-squares solution of the system of Eq. (10) for the phase calibration factors $\hat{\boldsymbol{\phi}}=[\hat{\phi}_1,\hat{\phi}_2,\ldots,\hat{\phi}_N]^{\mathrm{T}}$ follows from multiplying the vector of measured phase differences $\boldsymbol{v}=[v_1,v_2,\ldots,v_{N-2}]^{\mathrm{T}}$ by the pseudo-inverse of the coefficient matrix $\mathbf{C}$,

$$\hat{\boldsymbol{\phi}}=\mathbf{C}^{+}\boldsymbol{v} \tag{11}$$

where, from Eq. (10), $\mathbf{C}$ is a $(N-2)\times N$ banded matrix of the form,

$$\mathbf{C}=\begin{bmatrix} 1 & -2 & 1 & 0 & \ldots & \ldots & 0 \\ 0 & 1 & -2 & 1 & 0 & \ldots & \vdots \\ \vdots & \ddots & \ddots & \ddots & \ddots & \ddots & \vdots \\ \vdots & \vdots & \ddots & 1 & -2 & 1 & 0 \\ 0 & 0 & \ldots & 0 & 1 & -2 & 1 \end{bmatrix} \tag{12}$$

Finally, the cross-spectral matrix of pressure measurements, $\hat{\mathbf{S}}_{pp}$, corrected for phase calibration factors is given by

$$\hat{\mathbf{S}}_{pp}=\hat{\boldsymbol{\Gamma}}\tilde{\mathbf{S}}_{pp}\hat{\boldsymbol{\Gamma}}^{H} \tag{13}$$

where

$$\hat{\boldsymbol{\Gamma}}=\mathrm{diag}(\mathrm{e}^{-\mathrm{i}\hat{\phi}_1},\mathrm{e}^{-\mathrm{i}\hat{\phi}_2},\ldots,\mathrm{e}^{-\mathrm{i}\hat{\phi}_N}) \tag{14}$$

Calibration of the phase factors in an axial hydrophone array performed using Eq. (11) was proposed by Sng and Li [7]. Their work was a specific formulation of the general technique proposed in an earlier paper by Paulraj and Kailath [8]. The Paulraj and Kailath method was based on precisely the same principle but using a larger system of equations obtained from the differences of *all* the elements of Eq. (9) where $i-j=k-l$. Note also that in the application proposed by Paulraj and Kailath, namely the calibration of hydrophones for under-water applications, the source of noise is a single plane wave arriving from a single direction in an environment in which reflections are usually weak (except in very shallow water). In the application proposed in this paper, however, the sound field is multimodal, that is waves arrive at the array from numerous different locations. Later in this paper we will investigate the effectiveness of both techniques for calibrating the phase of in-duct microphones.

Note from Eq. (12) that the rank of the coefficient matrix, $\mathbf{C}$, is $N-2$ and hence the system of equations is under-determined, as shown by Paulraj and Kailath [8]. Solving Eq. (11) using the pseudo-inverse is equivalent to minimising $\|\hat{\boldsymbol{\phi}}\|^2$ under the constraint that $\mathbf{C}^{+}\hat{\boldsymbol{\phi}}=\boldsymbol{v}$. The phase calibration obtained using Eq. (11) therefore minimises the variance of the phase term along the leading diagonal of Eq. (9). In the experimental validation in the following section this calculation is performed using a singular value decomposition approach.[1]

[1] Specifically, the `pinv` function in Mathworks MATLAB v7.5.0.342 (R2007b).

3. Experimental validation of the array calibration technique

3.1. Experimental method

In this section an experiment is described aimed at validating the Töplitz assumption made in this paper. Furthermore the phase calibration technique developed in Section 2 is used to compare the phase calibration factors obtained for an array of microphones measured *in situ* in a duct with those measured under free-field conditions.

Fig. 1 is a schematic of the experimental set-up. A 4.8 m long hard-walled, steel duct of internal diameter 0.4 m passing though the wall connecting a reverberation chamber and an anechoic chamber. The duct was surrounded by a thick panel coated with rubber-backed foam and sealed around the edges with putty to ensure good acoustic isolation between the two chambers.

3.1.1. Reverberation chamber

Broadband noise was generated in the reverberation chamber using two well separated 400 W loudspeakers driven by mutually incoherent white noise signals via two power-amplifiers. The white noise signals were pre-generated, pseudo-random sequences and stored onto two channels of a 24 channel hard-disk recorder.

The reverberation room has nonparallel, highly reflective walls and a volume of 131 m^3. This ensures that the sound field in the room, and hence the sound-field incident on the open end of the duct, is reasonably diffuse at the frequencies of interest in this investigation.

3.1.2. In-duct measurements

Fig. 2 is a photograph of the in-duct microphone array. Fifteen 7 mm electret microphones were mounted on a thin plate of size 50 mm × 400 mm. The microphones were positioned at the edge of the plate, with the centre of the microphone capsules separated 25 mm apart. This spacing corresponds to $\lambda/2$ at a frequency of 6800 Hz or a duct frequency of ka=25 (assuming a sound speed of 340 m s^{-1}). The microphone cables passed through small holes in the plate, and were affixed to the underside of the plate so as to minimise their effect on the sound field in the duct.

The microphone array was located along the bottom of the duct, and as close as possible to the duct wall. The first microphone in the array was positioned 1.2 m from the open end of the duct, so as to minimise the effect of reflections from the open end.

Each microphone was connected to a custom-made signal amplifier. The time series were sampled simultaneously using a 32 channel SONY DAT recorder at a sampling rate of 48 kHz with 16 bit resolution. The total recording time for each test was 1 min.

The cross-spectrum between each pair of microphones was computed at each discrete frequency point using a Welch spectral estimation algorithm comprising a 2048 point FFT, Hamming window and 50 percent overlap.

We start by verifying the assumption made in Section 2 that the measured cross-spectral matrix for the axial microphone array has a Töplitz structure. The cross-spectral matrix is then used in Eq. (13) to determine the phase calibration factors for each microphone. To assess the robustness and accuracy of the technique these phase calibration factors are compared to those obtained by comparison with a calibrated reference microphone. This calibration was

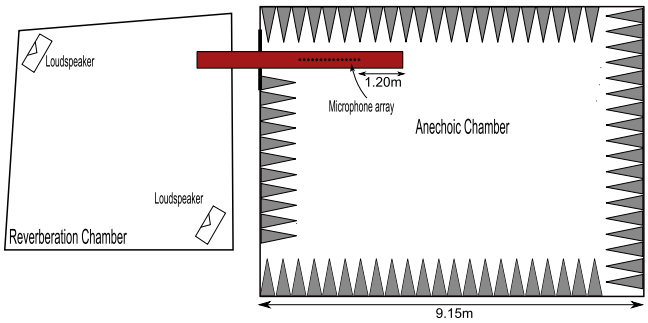

Fig. 1. A plan-view schematic of the experimental set-up. The reverberation chamber is connected to the anechoic chamber by a 4.8 m long steel duct with an internal diameter of 0.4 m. Noise is generated by loudspeakers in the reverberation chamber.

Fig. 2. A photograph of the in-duct microphone array. Fifteen 7 mm electret microphones were mounted on a thin 50 mm × 400 mm aluminium plate. The microphones were positioned at the edge of the plate, with the centre of the capsules 25 mm apart.

performed in an anechoic chamber by placing a B&K type 4185 microphone 5 mm away from the diaphragm of each of the array microphones in turn. White noise was generated with a loudspeaker, and the transfer function between the two microphones was measured. The produce was repeated four times with the loudspeaker in different positions and the average of the transfer function was taken.

3.2. Evidence for the Töplitz structure of $\mathbf{S}_{pp}$

The solid curve in Fig. 3 is a plot of measured phase difference, Φ_{ij}, as a function of normalised frequency $\Delta z/\lambda$ measured in the duct averaged over 14 adjacent pairs of phase-calibrated microphones 1.5 cm apart. The phase difference has been "unwrapped" (that is absolute jumps greater than π are changed to their 2π complement) for clarity of presentation. The error bars at each frequency represent plus and minus one standard deviation, σ_Φ, from the mean across the 14 phase estimates.

At frequencies below approximately $\Delta z/\lambda = 1$ (13.6 kHz, ka=50) the standard deviation, σ_Φ is less than 30°. The standard deviation at three particular frequencies is tabulated in Table 1. Below 5.4 kHz the variation in phase is less than 14° suggesting that below this frequency $\mathbf{S}_{pp}$ has the required Töplitz form to at least this level of accuracy. The random variation in the phase between adjacent microphones sets the limit for the accuracy of the phase estimate using Eq. (11). The standard deviation increases as frequency increases, and becomes very large for $\Delta z/\lambda > 0.85$. When the wavelength is smaller than the microphone separation distance the phase differences become significantly larger.

Fig. 4 plots the mean and standard deviation versus frequency for the phase differences of the second off-diagonal elements of $\mathbf{S}_{pp}$, that is for pairs of microphones separated 5 cm apart, that is, twice the distance of Fig. 3. This figure shows that below a normalised frequency of $\Delta z/\lambda = 1$ (6.8 kHz, ka=25) the standard deviation is approximately 20°, and increases dramatically for $\Delta z/\lambda > 0.85$.

In decreasing order of importance, deviation from Töplitz behaviour of $\mathbf{S}_{pp}$ measured in the duct arises from:

- Random errors in the phase estimates caused by poor coherence between microphones, particularly between those furthest apart.
- Correlation between individual modes in the duct, caused by reflections from the open end at $ka < 1$ and at the modal cutoff frequencies or the noise sources in the reverberation chamber.
- Uncorrelated noise at the microphones.

Piersol [9] has shown that the phase spectrum between two measurements for which the coherence is γ^2 has a variance of

$$\sigma_\Phi^2 \approx \frac{1-\gamma^2}{2r\gamma^2} \tag{15}$$

where r is the number of data segments used in the phase estimate.

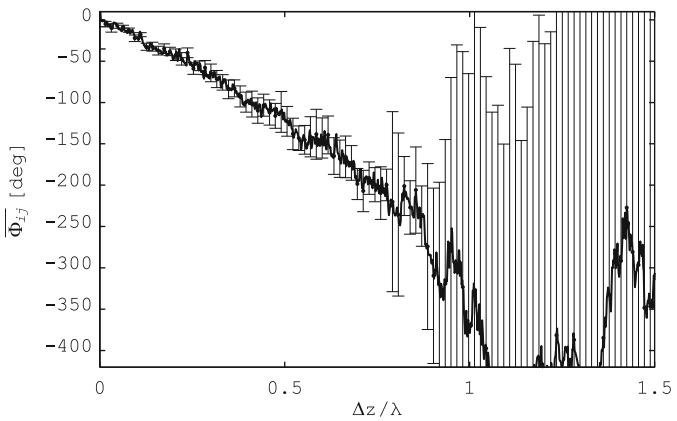

Fig. 3. Mean and standard deviation of the phase angle between adjacent microphones in a duct when $\Delta z = 2.5$ cm. Statistics based on 15 microphones.

Table 1
Standard deviation of the measured phase in Fig. 3.

Frequency (Hz)	Frequency (ka)	σ_Φ (deg)
2750	10	7
5490	20	14
8225	30	21

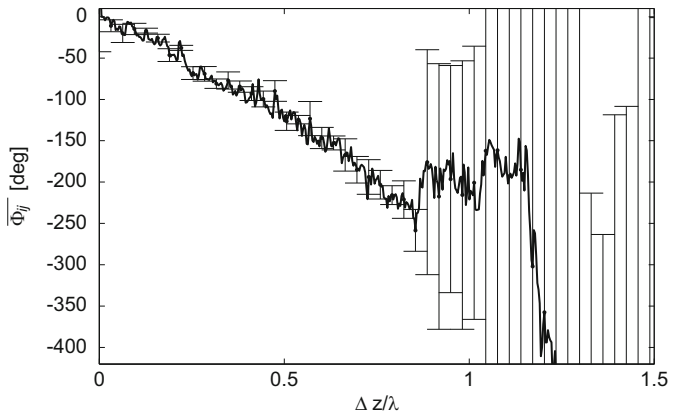

Fig. 4. Mean and standard deviation of the phase angle between adjacent microphones in a duct when $\Delta z = 5$ cm. Statistics based on eight microphones.

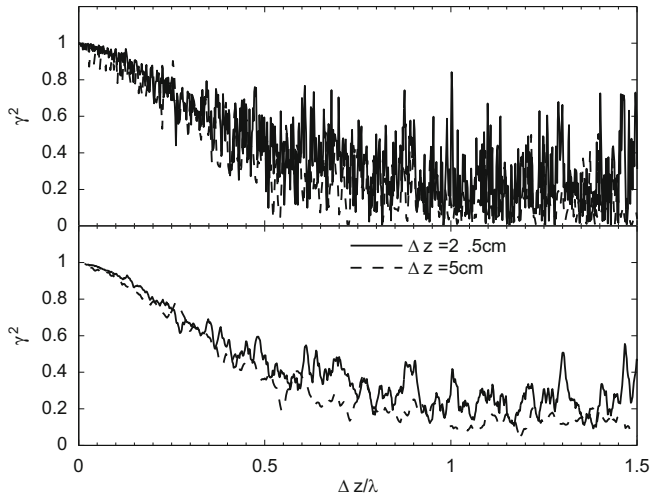

Fig. 5. Measured coherence between a pair of microphones separated by 2.5 cm (solid line) and 5 cm (dashed line) as a function of $\Delta z/\lambda$. The upper plot is obtained from the raw data, the lower plot is processed with a 200 Hz moving average.

The number of segments r may be approximated by $r \approx B_e T$, which when substituted into Eq. (15) reveals explicitly the dependence on phase variance on effective frequency bandwidth B_e and the sampling time T. Thus, random errors in the phase estimate may be reduced by increasing either B_e (by the use of a shorter window length) and/or the total data length T. An entirely equivalent method of increasing B_e and therefore reducing σ_Φ^2 is to average the phase estimates over a small frequency band so that each frequency point is obtained from a moving average. In the present investigation the $B_e T$ product was chosen to ensure convergence of the spectral estimates.

Eq. (15) also suggests that the phase calibration technique is likely to be inaccurate for microphone separation distances greater than approximately $\lambda/2$ since it is well known that the coherence, γ^2, between two microphones in a multimode broadband sound field tends to zero, leading to large random errors in the measured phase spectrum. Fig. 5 shows the coherence, as a function of $\Delta z/\lambda$, between a pair of microphones separated by 2.5 cm and a pair separated by 5 cm. The upper plot is obtained from the raw data, the lower plot is smoothed with a 200 Hz moving average window, as discussed above. The coherence can be seen to drop to approximately 0.2 at $\Delta z/\lambda = 0.85$ for both separation distances. This, and the large variability shown in the upper plot, causes σ_Φ^2 in Eq. (15) to become large above this frequency (or separation distance), as seen in Figs. 3 and 4.

3.3. Application of the calibration technique to the in-duct microphone array

Fig. 6 is a plot of the free-field measured phase calibration factors relative to microphone 1 as a function of frequency for microphones 1, 3, 5 and 11, as described in Section 3.1.2. The phase calibration factors below 12 kHz are observed to differ by up to 50° between different microphones.

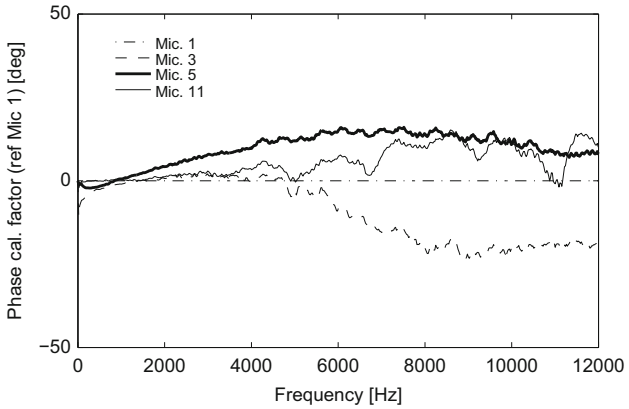

Fig. 6. A plot of the free-field measured phase calibration factors relative to microphone 1 as a function of frequency for microphones 1, 3, 5 and 11.

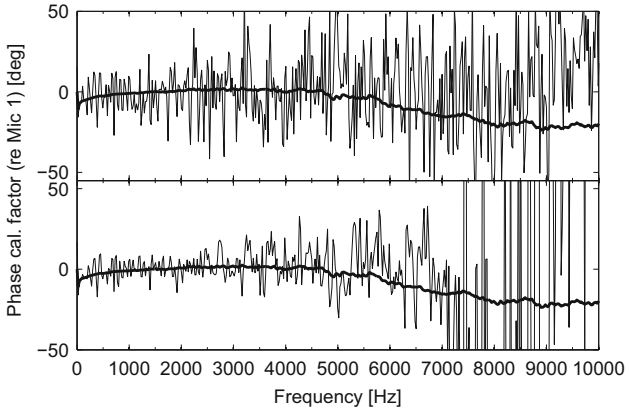

Fig. 7. A plot of the phase calibration factors as a function of frequency for microphone 3 obtained using the Paulraj (top) and Sng (bottom) methods. The thick line is the free-field measured phase factor, the thin line is the phase factor obtained using the *in situ* calibration technique.

Fig. 7 is a plot obtained from Eq. (11) of the phase calibration factors of microphone 3 as a function of frequency using the Paulraj (top) and Sng (bottom) methods. The Sng method (which uses just the first off-diagonal elements of the cross-spectral matrix) is observed to agree with the phase factors measured directly in Fig. 6 to within 10° up to approximately 4 kHz. Above this frequency the deviation of the inferred phase calibration factors from the measured phase calibration factors is appreciably greater, although the mean trend of the measured curve is reasonably well captured. Note that the deviations in the phase calibration factors obtained are comparable to those in Table 1, corresponding to the variance of the phase difference between adjacent microphones. The Paulraj method, which uses all the diagonals of the cross-spectral matrix, $\mathbf{S}_{pp}$, performs less well than the Sng method, computing phase calibration factors to within a few degrees only up to approximately 1000 Hz. Random fluctuations of the phase estimate about the mean are also significantly greater with the use of all diagonals.

As discussed in Section 3.2 the pressure cross-spectral matrix using calibrated sensors has a form closer to a Töplitz structure for diagonals close to the leading diagonal, i.e. for pairs of microphones that are closest together. Since the Paulraj method uses all diagonals in $\mathbf{S}_{pp}$, the phase calibration factors are contaminated by the data from those microphone pairs with large separation distances and therefore poor coherence. The method proposed by Sng uses only the first diagonal of $\mathbf{S}_{pp}$, and hence unlike the Paulraj method, does not use data from microphones separated by more than a wavelength for a wider range of frequencies.

Figs. 8 and 9 are plots of the phase calibration factors for microphones 5 and 11 obtained using both methods. The Sng method recovers the general trend with frequency of the phase calibration factors more closely than the Paulraj method in both cases.

The random fluctuations with frequency present in phase calibration factors in Figs. 7–9 may be significantly reduced by performing a moving-frequency average. This approach is justified since the phase calibration factors to be obtained can be assumed to be relatively slowly varying with frequency. Fig. 10 is a plot of the phase calibration factors after the application of a 10 point moving average, corresponding to a frequency bandwidth of 200 Hz. This process removes some of

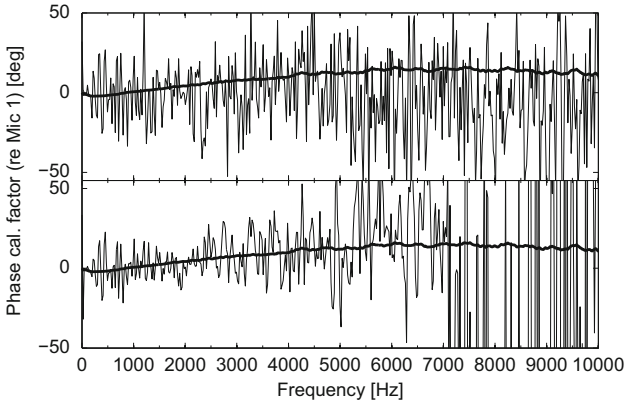

Fig. 8. As Fig. 7 but for microphone 5.

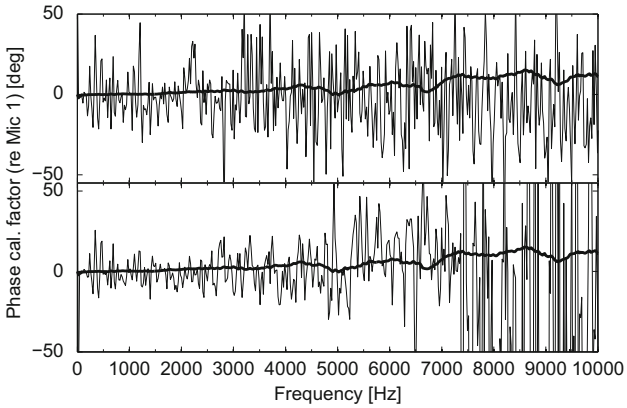

Fig. 9. As Fig. 7 but for microphone 11.

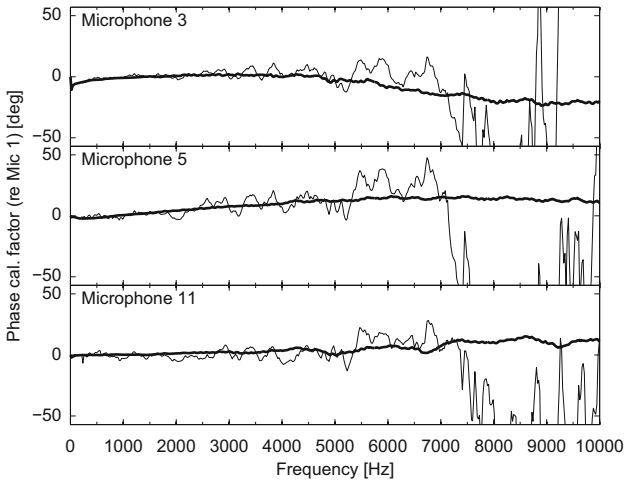

Fig. 10. A plot of the phase calibration factors as a function of frequency obtained using the Sng method (thin line) compared to those obtained in the free-field (thick line) for microphone 3 (top), 5 (middle) and 11 (bottom). The data is processed using a 10 point (200 Hz) moving average.

the variability from the data and allows the underlying trend to be more easily seen. The variation of phase calibration with frequency has been well captured for each microphone up to a frequency of approximately 5000 Hz.

The most significant source of error in this technique is the deviation of the cross-spectral pressure matrix from perfect Töplitz structure. The departure from Töplitz structure in phase is of the same magnitude as the phase calibration factors

we wish to determine using the technique, as shown in Fig. 3, that is approximately 7° at 2750 Hz and 14° at 5490 Hz. Calibration of the microphones to greater accuracy than this is therefore not possible.

4. Conclusions

In this paper a technique has been proposed to allow the phase calibration of the microphones used in in-duct axial arrays. The advantage of this technique over simple free-field calibration is that it allows the array to be calibrated rapidly *in situ*.

The technique is an extension of the SONAR linear array calibration technique proposed by Paulraj et al. [8] and Sng et al. [7]. The technique has been extended to linear arrays in ducts where the sound field is strongly multimodal with random phase fluctuations between modes and influenced by reflections from the open end of the duct. This paper contains the first experimental comparison of both methods. The Sng method has been shown to perform better than the Paulraj method on the experimental data tested.

Acknowledgments

This work was partly funded by Rolls-Royce plc through their University Technology Centre at Southampton University. The work benefited greatly from discussions with, and the technical expertise of Dr. Keith Holland of the ISVR.

References

[1] L. Enghardt, A. Holewa, U. Tapken, Comparison of different analysis techniques to decompose a broad-band ducted sound field in its mode constituents, *13th AIAA/CEAS Aeroacoustics Conference*, Rome, Italy, AIAA-2007-3520, 2007.
[2] U. Bolleter, M. Crocker, Theory and measurement of modal spectra in hard-walled cylindrical ducts, *Journal of the Acoustical Society of America* 51 (5) (1972) 1439–1447.
[3] P. Sijtsma, Feasibility of in-duct beamforming, *13th AIAA/CEAS Aeroacoustics Conference*, Rome, Italy, AIAA-2007-3696, 2007.
[4] C. Lowis, P. Joseph, A. Kempton, An in-duct beamformer for the estimation of far-field directivity, *14th AIAA/CEAS Aeroacoustics Conference*, Vancouver, BC, Canada, 2008.
[5] J. Lavrentjev, M. Åbom, H. Bodén, A measurement method for determining the source data of acoustic two-port sources, *Journal of Sound and Vibration* 183 (3) (1995) 517–531.
[6] F.O. Castres, P.F. Joseph, Experimental investigation of an inversion technique for the determination of broadband duct mode amplitudes by the use of near-field sensor arrays, *Journal of the Acoustical Society of America* 122 (2) (2007) 848–859.
[7] Y. Sng, Y. Li, Fast algorithm for gain and phase error calibration of linear equi-spaced (LES) array, *Proceedings of ICSP2000*, 2000.
[8] A. Paulraj, T. Kailath, Direction of arrival estimation by eigenstructure methods with unknown sensor gain and phase, *Proceedings of the IEEE International Conference on Acoustics, Speech, and Signal Processing, ICASSP 85*, Cat. no. 85CH2118-8, 1985, pp. 640–643.
[9] A. Piersol, Time delay estimation using phase data, *IEEE Transactions on Acoustics, Speech and Signal Processing* 29 (3) (1981) 471–477.